doi:10.1093/brain/awx073 BRAIN 2017: 140; 1692–1705 | 1692

BRAIN
A JOURNAL OF NEUROLOGY

Imaging blood–brain barrier dysfunction as a biomarker for epileptogenesis

Guy Bar-Klein,[1,†] Svetlana Lublinsky,[1] Lyn Kamintsky,[2] Iris Noyman,[3,4] Ronel Veksler,[1] Hotjensa Dalipaj,[2] Vladimir V. Senatorov Jr.,[5] Evyatar Swissa,[1] Dror Rosenbach,[1] Netta Elazary,[1] Dan Z. Milikovsky,[1] Nadav Milk,[6] Michael Kassirer,[6] Yossi Rosman,[6,7] Yonatan Serlin,[2] Arik Eisenkraft,[6,8,9] Yoash Chassidim,[1] Yisrael Parmet,[10] Daniela Kaufer[5,*] and Alon Friedman[1,2,*]

*These authors contributed equally to this work.

A biomarker that will enable the identification of patients at high-risk for developing post-injury epilepsy is critically required. Microvascular pathology and related blood–brain barrier dysfunction and neuroinflammation were shown to be associated with epileptogenesis after injury. Here we used prospective, longitudinal magnetic resonance imaging to quantitatively follow blood–brain barrier pathology in rats following status epilepticus, late electrocorticography to identify epileptic animals and post-mortem immunohistochemistry to confirm blood–brain barrier dysfunction and neuroinflammation. Finally, to test the pharmacodynamic relevance of the proposed biomarker, two anti-epileptogenic interventions were used; isoflurane anaesthesia and losartan. Our results show that early blood–brain barrier pathology in the piriform network is a sensitive and specific predictor (area under the curve of 0.96, $P < 0.0001$) for epilepsy, while diffused pathology is associated with a lower risk. Early treatments with either isoflurane anaesthesia or losartan prevented early microvascular damage and late epilepsy. We suggest quantitative assessment of blood–brain barrier pathology as a clinically relevant predictive, diagnostic and pharmaco!dynamics biomarker for acquired epilepsy.

1 Departments of Physiology and Cell Biology, Brain and Cognitive Sciences, Zlowotski Center for Neuroscience, Ben-Gurion University of the Negev, Beer-Sheva, Israel
2 Department of Medical Neuroscience, Dalhousie University, Halifax, Nova Scotia, Canada
3 Pediatric Neurology and Epilepsy, Pediatric Division, Soroka Medical Center, Beer-Sheva, Israel
4 Faculty of Health Sciences, Ben-Gurion University of the Negev, Beer-Sheva, Israel
5 Department of Integrative Biology and the Helen Wills Neuroscience Institute, University of California, Berkeley, California, USA
6 The Israel Defense Force Medical Corps, Tel Hashomer, Israel
7 Sackler School of Medicine, Tel Aviv Uneversity, Tel Aviv, Israel
8 NBC Protection Division, Ministry of Defense, Tel-Aviv, Israel
9 The Institute for Research in Military Medicine, Hebrew University, Jerusalem, Israel
10 Department of Industrial Engineering and Management, Ben-Gurion University of the Negev, Beer-Sheva, Israel

†Present address: Howard Hughes Medical Institute and the Institute of Genetic Medicine, Johns Hopkins University School of Medicine, 733 N. Broadway, Baltimore, MD, 21205, USA

Correspondence to: Prof. A. Friedman,
Ben-Gurion University of the Negev, P.O.box 653, Beer-Sheva, Israel 8410501
E-mail: alonf@bgu.ac.il

Keywords: biomarker; epilepsy; blood–brain barrier; magnetic resonance imaging

Abbreviations: BBB = blood–brain barrier; ECoG = electrocorticography

Received July 13, 2016. Revised January 24, 2017. Accepted January 31, 2017. Advance Access publication April 23, 2017

Introduction

In the field of brain protection and therapeutics, phase III clinical trials have repeatedly failed to show therapeutic efficacy. This has necessitated a re-examination of translational research in this area. A growing consensus holds that, in addition to better understanding of underlying disease mechanisms, there is also a need for biomarker-driven strategies to identify patients with specific brain pathobiological processes increasing the risk for a brain disorder, confirm engagement of the proposed molecular target by the therapeutic agent and provide quantitative measures to assess therapeutic efficacy. The goal of biomarker research is thus to facilitate clinical studies by enabling rationalized subject selection, dosing, timing, and duration of treatment. In the field of post-injury epilepsy, no such biomarker is currently available (Cendes, 2012; Engel *et al.*, 2013; Friedman *et al.*, 2014; Pitkänen *et al.*, 2016).

Cerebral microvascular pathology (microvasculopathy) is a frequent feature of the injured brain, with dysfunction of the blood–brain barrier (BBB) as one prominent hallmark (Abbott *et al.*, 2006; Kenney *et al.*, 2016). A compromised BBB is also found in epileptic brain tissue (Oby and Janigro, 2006; van Vliet *et al.*, 2007) and in patients with post-traumatic epilepsy (Tomkins *et al.*, 2008). BBB dysfunction occurs early in kainic acid model of status epilepticus and correlates with the seizures frequency in the chronic stage (van Vliet *et al.*, 2014). Experimental BBB breakdown induces rewiring of brain networks and epilepsy (Seiffert *et al.*, 2004; Bar-Klein *et al.*, 2014*a*) through brain exposure to serum albumin (Ivens *et al.*, 2007; Bar-Klein *et al.*, 2014*a*; Weissberg *et al.*, 2015; van Vliet *et al.*, 2016*a*). Albumin binds to transforming growth factor β (TGF-β) receptor II in astrocytes and activates the activin-like kinase 5 pathway, leading to phosphorylation of its intracellular messengers (Smad2/3) (Cacheaux *et al.*, 2009; Bar-Klein *et al.*, 2014*a*) and a transcriptional response resulting in astroglial dysfunction, neuroinflammation, downregulation of GABA-related genes, and excitatory synaptogenesis (Ivens *et al.*, 2007; David *et al.*, 2009; Levy *et al.*, 2015; Weissberg *et al.*, 2015). It therefore stands to reason that microvasculopathy is likely responsible, at least in part, for neural dysfunction and post-injury epilepsy, making brain vasculature an attractive biomarker and therapeutic target after insults to the brain.

Our goal was to test the potential of a quantitative BBB imaging as a pathobiologically relevant biomarker for identifying the 'epileptogenic brain tissue', predict the development of epilepsy and serve as a pharmacodynamic biomarker to assess the efficacy of novel treatments. We have thus designed our study with the following aims: (i) to develop a clinically relevant animal model that is likely to induce epileptogenesis but with a diverse outcome, in which only ~50% of the animals develop epilepsy; (ii) to develop and validate clinically relevant imaging methods to detect and quantify BBB dysfunction; (iii) to challenge the hypothesis that early BBB dysfunction predicts the development of epilepsy; and (iv) to explore the use of BBB dysfunction as a pharmacodynamic biomarker. We used MRI protocols and electrocorticographic (ECoG) recordings in a modified rat model of paraoxon-induced epileptogenesis (Todorovic *et al.*, 2012; Bar-Klein *et al.*, 2014*b*). Paraoxon is a commonly used pesticide and a frequent cause of seizures due to accidental intoxication (most often in developing countries) (Cehovic *et al.*, 1972; Marrs, 1993) and has been recently shown as a reliable model for status epilepticus-induced epileptogenesis in the rat (Shrot *et al.*, 2014). We report that quantitative assessment of vascular injury can serve as a diagnostic, predictive and pharmacodynamics biomarker for epilepsy. Finally, we illustrate the feasibility of contrast-enhanced MRI for the quantitative assessment of BBB pathology in the clinical scenario.

Material and methods

Experimental design

We modified the established paraoxon-induced status epilepticus model by pharmacologically terminating the status after 30 min. We next developed three MRI protocols and quantitative analysis methods for the detection of abnormal magnetic resonance signals in 13 segmented brain regions. Rats were randomly assigned into naïve (controls) and paraoxon-treated groups. Our experience, based on previously acquired data, showed that neocortical seizures and general tonic-clonic convulsions before Week 4 after poisoning were rarely documented. However, once animals develop epilepsy, recurrent seizures persist as long as the recordings continued. Therefore, in this study rats were scanned at 2 days (early epileptogenesis), 1 week (late epileptogenesis) and 1 month (after epilepsy developed) following status epilepticus. An experimenter blinded to the treatment performed all data analysis. After magnetic resonance scans, rats ($n = 22$) were monitored for epilepsy 5–7 weeks after exposure, using continuous (24/7) video-ECoG. The major outcome measure (development of epilepsy) was determined using an automated seizure detection algorithm, allowing classification of animals as epileptic if spontaneous seizures were detected. Each animal was given a code and the experimenter was blinded to treatment during ECoG analysis. Using this binary determination, we analysed the extent of abnormal magnetic resonance signal in each brain region using logistic regression and forward selection with a 'leave one out' procedure. Three control groups were included in our experiments: (i) control animals with no additional treatment; (ii) animals with 'anaesthesia treatment' that were provided with repetitive isoflurane anaesthesia, a documented treatment of refractory status epilepticus and an epileptogenesis-modifying treatment (Bar-Klein *et al.*, 2016); and (iii) animals with 'losartan treatment', which were provided with

intraperitoneal adminstration (60 mg/kg) once every 24 h for 3 days followed by oral treatment (2 g/l in the drinking water) for an additional 18 days. Losartan is an angiotensin receptor antagonist also shown to antagonize TGF-β signalling, used as an anti-inflammatory and neuroprotective drug (Campistol *et al.*, 1999; Ongali *et al.*, 2014), and reported to suppress epileptogenesis in BBB and albumin models of epilepsy (Bar-Klein *et al.*, 2014*a*).

The sample sizes chosen were adequately powered to observe the effects based on previous studies from our group using the same treatment protocols (Bar-Klein *et al.*, 2014*b*; Shrot *et al.*, 2014). The experimenters were blind to the treatment during the experiments and initial data analysis (seizure detection and image analysis). All data are included (no outlier values were excluded).

Reagents

Paraoxon, atropine, propylene glycol, Evans blue and Triton™ X-100 were purchased from Sigma Aldrich. Toxogonin (obidoxime chloride) was obtained from Merck Sereno, midazolam from Rafa Laboratories Ltd.; gadoteric acid (Dotarem®) from Guerbet; and Gadofosveset trisodium (Ablavar®) from Lantheus Medical Imaging.

Animal preparation

All experimental procedures were approved by the Animal Care and Use Ethical Committees at the Ben-Gurion University of the Negev, Beer-Sheva, Israel, and were conducted in adherence to the NIH Guide for the Care and Use of Laboratory Animals. Experimental animals were obtained from Harlan Laboratories and were kept under a 12:12 h light-dark routine, and supplied with drinking water and food *ad libitum*.

Ninety-nine adult male Sprague-Dawley rats (300–325 g) were treated with paraoxon (intramuscular, 0.45 mg/kg, equivalent to 1.4 LD_{50}) dissolved in propylene glycol and saline (at a ratio of 1:27.25) to induce status epilepticus. To reduce the peripheral effects of paraoxon and prevent mortality, 1 min after treatment rats were treated with atropine and toxogonin (intramuscular, 3 and 20 mg/kg respectively, in saline). Midazolam was administered (intramuscular, 1 mg/kg) 30 min following exposure to paraoxon (Shrot *et al.*, 2014).

MRI

MRI was performed in midazolam-treated rats. In the first series of experiments, scans were performed in naïve (n = 16) and treated (n = 42) rats at intervals of 2 days, 1 week and 1 month. In the second series of experiments, scans were performed every 1, 6 and 12 h, and every 1, 2 and 3 days, as well as 1 week and 1 month following status epilepticus (n = 8). Scans were performed using the Aspect M2 system (Aspect Imaging Technologies) under isoflurane anaesthesia (1–2%) with a constant oxygen flow (99%, 1 l/h). Breathing was monitored continuously during imaging using a respiration monitor (Aspect Imaging Technologies).

Scanning protocols included: (i) T_1-weighted spin echo classic scans (repetition time/echo time/number of excitations = 400/14/2 ms, with acquisition time of 2.5 min), performed before and after the injection of the gadolinium-based tracers (gadoteric acid or gadofosveset trisodium, IM, 0.5 mmol/kg) as previously established (Chassidim *et al.*, 2013); (ii) standard T_2-weighted fast spin echo sequence (repetition time/echo time/number of excitations = 3400/74/4 ms, with acquisition time of 14.5 min); and (iii) diffusion-weighted imaging (DWI) sequences (repetition time/echo time = 1500/22.5 ms, with acquisition time of 12.5 min). The scans were collected with a 5 cm field-of-view and data matrix of 256 × 256, resulting in a 0.195 mm in-plane resolution and slice thickness of 1 mm.

Analysis of the images was performed using in-house Matlab scripts. Images first underwent preprocessing to extract the brain volume of interest and the creation of enclosed 3D brain objects. Images were then registered to a rat brain atlas (LONI Laboratory of Neuro Imaging, http://www.loni.usc.edu/atlases), enabling the automatic segmentation into anatomical brain regions. Signal changes, reflecting a compromised BBB, were measured in 13 brain regions (comprising 91% of the scanned brain): the amygdala, corpus callosum, fimbria fornix, hindbrain, hippocampus, internal capsule, midbrain, neocortex, pallidum, piriform network (included here the olfactory bulbs, piriform cortex, dorsal endopiriform nucleus and inferior olive), septum, striatum and thalamus. For each region, the percentage of voxels, with apparent BBB dysfunction, was calculated using three different methods.

T_1-weighted contrast enhancement

Contrast-enhanced imaging is the most common approach to assess BBB integrity *in vivo*. Enhancement was determined by calculating the per cent difference between pre- and post-contrast scans (Chassidim *et al.*, 2013). Based on normal distribution of enhancement in naïve animals, voxels within the enhancement range of 30–100% were considered to represent brain tissue with a compromised BBB [with voxels enhanced over 100% corresponding to blood vessels (Chassidim *et al.*, 2015)]. A region-growing procedure was applied to BBB-compromised voxels, involving repeatedly connecting neighbouring voxels with an enhancement range of 20–30% to the seed object until the final growth was achieved. Small noisy clusters (less than four neighbouring voxels) were removed using a morphological filtering procedure.

T_2-weighted signal

An abnormal T_2-weighted signal was used to reflect the accumulation of water molecules (i.e. oedema; Gerriets *et al.*, 2004). Hyperintense voxels from brain volumes of interest were defined using the finite Gaussian mixture model. The observed variability of intensities could be

described as a mixture of three Gaussians, namely: 'low' (mostly representing white matter), 'medium' (grey matter) and 'high' (ventricles or abnormally hyperintense regions). Small, noisy clusters were removed, as described above.

Abnormal signal in apparent diffusion coefficient maps

Apparent diffusion coefficient (ADC) maps were calculated from five different b-values (i.e. 50, 200, 600, 800, and 1100 s/mm^2) based on DWI sequences. High or low ADC thresholds were defined as mean (μ) $\pm$ standard deviation (σ) of the ADC value distribution in naïve rats ($n = 16$, Gaussian distribution).

Ex vivo assessment of blood–brain barrier permeability

Two approaches were used to confirm BBB dysfunction in regions with abnormal MRI signals: Evan's blue was injected to the tail vein ($n = 4$, 48 mg/kg). Rats were deeply anaesthetized 30 min later and perfused with phosphate-buffered saline (PBS) containing 4% paraformaldehyde (PFA). Brains were then removed and coronal slices (1-mm thick) were obtained and imaged for Evan's blue extravasation. Immunohistochemistry was also performed to detect extravasation of serum albumin and IgG, as well as any local inflammatory responses.

For immunohistochemistry, rats were deeply anaesthetized and perfused with PBS containing 4% PFA. Brains were then removed and fixed overnight (4% PFA, 4°C), and were cryoprotected with sucrose gradient (10% followed by 20 and 30% sucrose in PBS). Coronal sections (30-µm thick) were obtained using a freezing microtome (Leica Biosystems). Immunofluorescence was performed in the free-floating sections against albumin (Abcam ab106582, followed by Donkey anti-chicken IgY Cy3, Millipore AP194C), IgG (goat anti-rat IgG-FITC conjugated, Sigma F6258), GFAP (Dako Z0334, followed by donkey anti-rabbit IgG-Alexa Fluor® 488, ThermoFisher Scientific, A21206) and ionized calcium binding adaptor molecule 1 (IBA-1, Wako 019-19741, followed by donkey anti-rabbit IgG-Alexa Fluor® 488, ThermoFisher Scientific, A21206). The dilution for both the primary and the secondary antibodies was 1:500. DAPI staining was performed with ProLong® Diamond Antifade Mountant containing DAPI (Invitrogen P36962). Cresyl violet (ICN 10510-54-0) was used for Nissl staining. Sections were visualized with either Zeiss Axioplan II MOT or Zeiss Axio Obzerver Z1.

Electrocorticographic recordings and seizure detection

Electrode implantation, recording and analysis were performed as described (Bar-Klein *et al.*, 2014*a*, *b*). In short, epidural electrodes were implanted 3 mm caudal and 2.5 mm lateral to bregma (i.e. one on each hemisphere) under deep ketamine and xylazine anaesthesia (intraperitoneal, 80 and 5 mg/kg, respectively). A telemetric transmitter (CTA-F40 or CA-F40, Data Science International) was implanted subcutaneously. Rats were then given a 4–7-day recovery period before initiation of ECoG recordings (1 kHz sampling rate) for 2 weeks starting from the fifth week after status epilepticus (14 consecutive days, 24 h a day). ECoG analysis was performed blindly (i.e. the experimenter was not aware of the treatment) using an in-house automated seizure detection algorithm, based on feature extraction and artificial neural network (ANN) clustering. Seizures were defined as events lasting a minimum of 5 s, thus a sliding window thresholding procedure was used to detect consecutive 'positive' ANN outputs. System performance was evaluated by analysing over 2800 h of ECoG signal from three epilepsy models; pilocarpine, albumin and synapsin triple knockout. Performance assessment resulted in overall sensitivity and positive predictive value above 98% (for more details see Bar-Klein *et al.*, 2014*a*). As an additional precautionary measure, all positively identified seizures were examined by an expert.

Statistical analysis

Differences in MRI findings, in each of the selected brain regions, were tested using the Mann-Whitney test, with Benjamini–Hochberg false discovery rate correction (BH step-up procedure) (SPSS, IBM, Armonk, NY, USA). To identify brain regions with positive and negative predictive values for the risk to develop epilepsy, logistic regression and forward selection were used. A 'leave one out' procedure was used to assess the performance of the model (R environment, the GNU project). To evaluate the quality of the proposed MRI biomarker, receiver operating characteristic (ROC) analysis was carried (Matlab, Mathworks Inc., Natick, MA, USA). The differences in per cent of animals presenting distinct epileptic seizures in non-anaesthetized, anaesthetized and losartan treated rats were analysed using Fisher's exact test (due to small cell sizes). $P \leqslant 0.05$ was determined as the statistical significance level.

Results

Midazolam shortens status epilepticus and results in a novel epilepsy model with a heterogeneous outcome

Consistent with previous studies (Bar-Klein *et al.*, 2014*b*; Shrot *et al.*, 2014), paraoxon injection (1.4 LD50) resulted in prolonged (5.35 $\pm$ 1.86 h) status epilepticus, manifested as generalized tonic-clonic convulsions (stage 5, according to the Racine scale; Racine, 1972) in all rats. The end of status epilepticus was defined as the last stage 5 seizure.

Spontaneous seizures were recorded at Weeks 5–7 in 85.7% (six of seven) of the rats. Status epilepticus was shortened (to 0.44 ± 0.4 h, $P < 0.0001$, Mann-Whitney test) using midazolam (1 mg/kg intramuscularly) injected 30 min after the appearance of clinical seizures. This protocol resulted in 59.1% (13 of 22, $P < 0.0001$, Fisher's exact test) animals with spontaneous seizures (lasting 54.43 ± 1.93 s) 5–7 weeks after poisoning (i.e. epileptic, Fig. 1A). There was no correlation between status epilepticus duration and delayed seizures within the group of midazolam-treated.

MRI confirms blood–brain barrier dysfunction following status epilepticus

To test whether paraoxon-induced epileptogenesis is associated with MRI-detectable microvasculopathy, we followed longitudinal changes in brain tissue that reflect a compromised BBB. Magnetic resonance scans were performed at three time points after status epilepticus, selected to reflect early pathology (Day 2), the latent period of

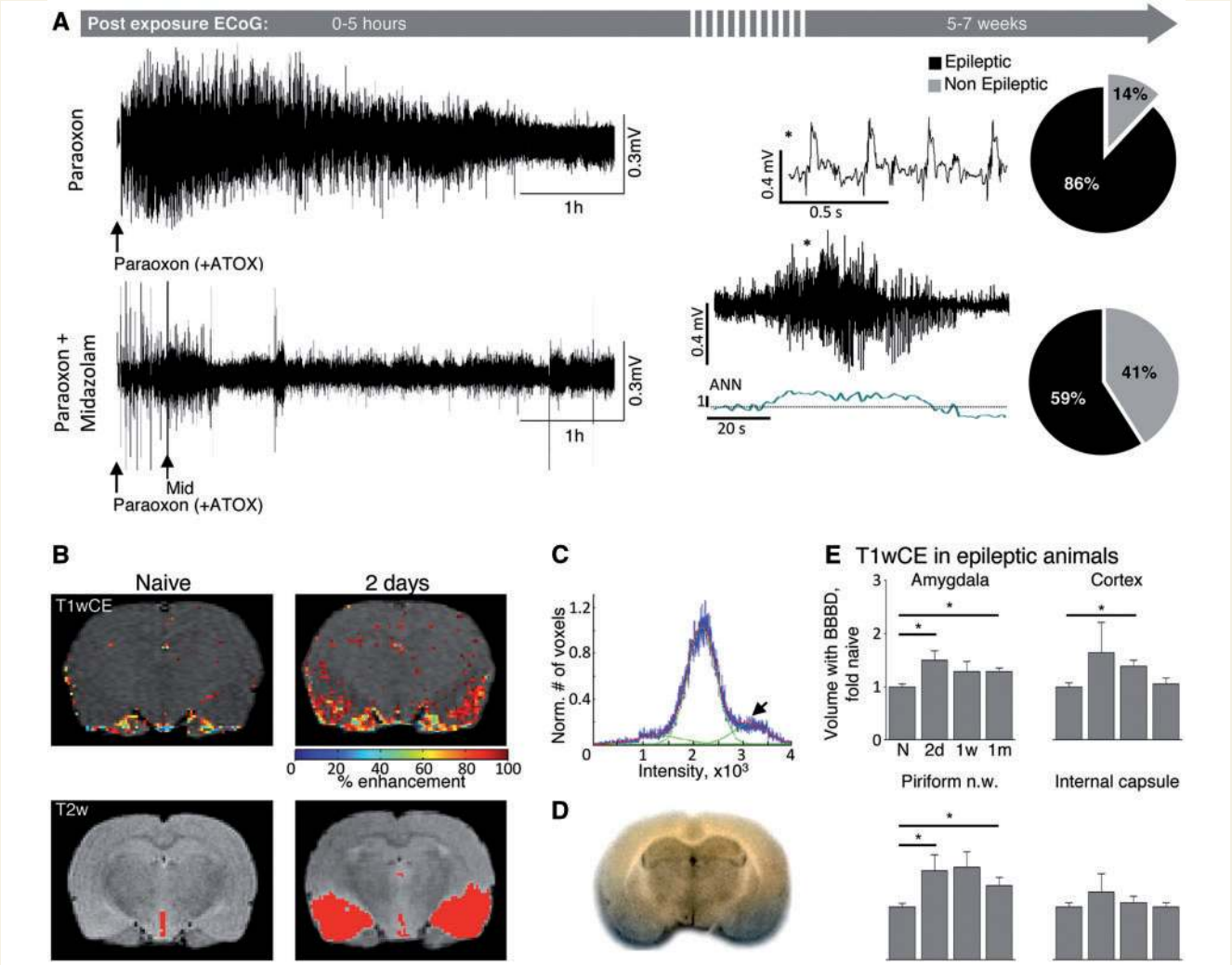

Figure 1 Imaging vascular integrity in a new model for status epilepticus-induced epilepsy. (**A**) To establish a novel model for epileptogenesis with a heterogeneous outcome we injected paraoxon [1.4 LD50, followed 1 min later by atropine and toxogonin (ATOX)] to induce status epilepticus. Treating rats with midazolam 30 min following exposure to paraoxon reduced the likelihood of epilepsy (⩾2 delayed spontaneous seizures) from 86% ($n = 7$) to 59% ($n = 22$). (**B**) Detection of BBB dysfunction using T_1-weighted contrast enhancement (T1wCE) and T_2-weighted magnetic resonance scans of naïve animals and at Day 2 following status epilepticus. Voxels with apparent BBB dysfunction detected using T_1-weighted contrast enhancement are colour coded (per cent enhancement after injection of the contrast agent) and superimposed on T_1-weighted images. Voxels characterized by abnormally high T_2 signal are coloured red and superimposed on T_2-weighted images. (**C**) The distribution of T_2-weighted signal intensities. A mixture of three Gaussian probability density functions was used to define 'abnormal (lesioned) voxel'. The lesion cut-off threshold was defined as an intersection between 2D and 3D Gaussians (arrow). (**D**) Brain removed 48 h after status epilepticus and 2 h after injection of Evan's blue, showing that extravasation of the dye is consistent with the increased magnetic resonance signal. (**E**) Changes in T_1-weighted contrast enhancement were found to be significantly higher in epileptic animals compared to naïve controls within specific brain regions. ANN = artificial neural network.

epileptogenesis (prior to the development of generalized seizures, 1 week) and after epilepsy is established (1 month) (Shrot *et al.*, 2014).

The acquired images underwent registration and segmentation into 13 brain subregions. Each voxel was characterized by four features portraying BBB dysfunction: (i) T_1-weighted contrast enhancement, reflecting brain accumulation of peripherally-injected contrast agent; (ii) abnormal T_2-weighted signal, reflecting changes in water content; (iii) high ADC; or (iv) low ADC maps, reflecting changes in water content and/or distribution within the neuropil. The percentage of volume within each subregion demonstrated by signal abnormalities was calculated for each time point and compared to the control group of un-exposed animals (naïve).

The MRI analysis of paraoxon-exposed rats ($n = 42$) compared to non-exposed controls (naïve, $n = 16$) revealed statistically significant higher T_1-weighted contrast enhancement signal in the neocortex and striatum at 1 week and in the amygdala, hippocampus, midbrain, piriform network (included the olfactory bulbs, piriform cortex, dorsal endopiriform nucleus and inferior olive), septum, striatum and thalamus at 1 month ($P < 0.05$, Fig. 1B and E). Abnormal T_2-weighted signal was found in exposed animals at all three time points in the majority of brain regions (Fig. 1C and D, and Table 1). No significant differences were found in DWI analysis between exposed and control animals.

To validate that the changes in MRI signal reflect a compromised BBB, rats ($n = 4$) were injected with the non-permeable albumin-binding dye, Evan's blue (intravenous, 48 mg/kg) 2 days after status epilepticus, and were subjected to microscopic analysis. Consistent with the MRI data, the piriform cortex and amygdala showed a prominent Evan's blue signal (Fig. 1D and see below).

Specific MRI features predict the development of epilepsy

To test if the observed changes in magnetic resonance signal predict epilepsy, we used ECoG monitoring ($n = 22$, weeks 5–7 after status epilepticus, recordings were not acquired later than the seventh week, which may result in missing seizures in animals with significantly delayed epileptogenesis) to identify 'epileptic' ($\geqslant$ two spontaneous seizures, $n = 13$) and 'non-epileptic' ($n = 9$) rats. Imaging results (percentage of voxels in each brain region with BBB dysfunction) were compared to non-exposed naïve ($n = 16$) rats. Epileptic animals presented a significantly higher T_1-weighted contrast enhancement in the

Table 1 MRI detected status epilepticus-induce brain abnormalities

Brain region	T_1-weighted contrast enhancement						T_2-weighted abnormal signal					
	2 days		1 week		1 month		2 days		1 week		1 month	
BBB dysfunction following status epilepticus (all animals)												
Amygdala	ns		ns		0.003		0.000		0.000		0.003	
Corp. cal.	ns		ns		ns		0.000		0.034		ns	
Hippocampus	ns		ns		0.003		ns		ns		ns	
Int. cap.	ns		ns		ns		0.000		ns		ns	
Midbrain	ns		ns		0.003		ns		ns		ns	
Neocortex	ns		0.013		ns		0.002		ns		ns	
Pallidum	ns		ns		ns		0.000		ns		ns	
Piriform n.w.	ns		ns		0.020		0.000		0.007		0.000	
Septum	ns		ns		0.022		0.050		0.009		0.000	
Striatum	ns		0.033		0.000		0.000		0.029		0.003	
Thalamus	ns		ns		0.016		ns		ns		ns	
BBB dysfunction is associated with increased risk for epileptogenesis												
	E	NE	E	NE	E	NE	E	NE	E	NE	E	NE
Amygdala	0.046	ns	ns	ns	0.022	ns	0.000	0.013	0.013	ns	0.007	0.007
Corp. cal.	ns	ns	ns	ns	ns	ns	0.007	0.036	ns	ns	ns	ns
Hippocampus	ns	ns	ns	ns	0.022	ns	ns	ns	ns	ns	ns	ns
Int. cap.	ns	ns	ns	ns	ns	ns	0.000	0.037	ns	ns	ns	ns
Neocortex	ns	ns	0.039	ns	ns	ns	0.000	ns	ns	ns	ns	ns
Pallidum	ns	ns	ns	ns	ns	ns	0.000	0.013	ns	ns	ns	ns
Piriform n.w.	0.046	ns	ns	ns	0.042	ns	0.000	0.022	0.013	ns	0.000	0.007
Septum	ns	ns	ns	ns	0.047	ns	ns	ns	0.026	ns	0.007	0.026
Striatum	ns	ns	ns	ns	0.022	ns	0.000	0.037	0.050	ns	0.007	ns

A significance table showing statistically significant changes in magnetic resonance T_1-weighted contrast enhancement and T_2-weighted abnormal signals in rats after status epilepticus compared to naïve rats (Mann-Whitney test with Benjamini–Hochberg false discovery rate correction) at 2 days, 1 week and 1 month by brain region. Note that while changes in T_2 abnormal signal characterize both groups, T_1-weighted contrast enhancement was significantly different only in epileptic rats. Brain regions with no significant differences in all time points were excluded from the table. Corp. cal. = corpus callosum; Int. cap. = internal capsul; Piriform n.w. = piriform network; ns = not significant (i.e. *P*-value > 0.05); E = epileptic; NE = non-epileptic.

amygdala and piriform network on Day 2 following status epilepticus, in the neocortex at 1 week and in the amygdala, hippocampus, piriform network, septum and striatum at 1 month ($P < 0.05$, Fig. 1E). At Day 2, epileptic rats also demonstrated a significantly increased T_2-weighted signal in the amygdala, corpus callosum, internal capsule, neocortex, piriform network, pallidum and striatum ($P < 0.05$). At 1 week and 1 month, increased T_2-weighted signal was found significant in the amygdala, piriform network, septum and striatum ($P < 0.05$). Importantly, non-epileptic animals did not show differences in T_1-weighted contrast enhancement, when compared as a group to naïve rats. T_2-weighted signal was significantly higher in non-epileptic animals at Day 2 in the amygdala, corpus callosum, internal capsule, pallidum, piriform network and striatum compared to naïve animals ($P < 0.05$). At 1 week no significant increase was measured and at 1 month, a significant increase was found in the amygdala, piriform network and septum ($P < 0.05$, Fig. 2A and B, and Table 1).

We next used a logistic regression model to search for brain region(s) with early BBB pathology that would best predict epilepsy. We used 26 variables (per cent voxels with abnormal T_2-weighted and T_1-weighted contrast enhancement signal in 13 brain regions, $n = 22$) from images obtained at Day 2 after exposure, with respect to the binary determination of epileptic or non-epileptic. Forward selection algorithm was used to create the model with a 'leave one out' performance evaluation. The procedure identified T_2-weighted signal increase in the piriform network [$\hat{\beta} = 2.83$, high values indicates for a higher probability (P) for epilepsy] as the most predictive for epilepsy. Using $P = 0.5$ as a cut-off point (for $P > 0.5$ the rat will be classified as epileptic) the sensitivity was 84.6% (11 of 13 epileptic rats were correctly classified), and specificity of 44.4% (five of nine non-epileptic rats were falsely classified). ROC analysis revealed an area under the curve (AUC) of 0.72 ($P = 0.089$, Fig. 2E). Interestingly, the statistical model also revealed brain regions, including the internal capsule, septum and thalamus ($\hat{\beta} = -0.475$, -2.951, -0.672, respectively), in which BBB dysfunction was associated with a lower probability for epilepsy. In fact, the statistical model identified both an 'epileptogenic network' (mainly the piriform network), in which BBB damage increased the risk for epilepsy, as well as a 'limiting network' (included the internal capsule, septum and thalamus), in which BBB damage reduced the risk for epilepsy. While BBB dysfunction within the epileptogenic network was found in all animals that later developed epilepsy, the non-epileptic group was heterogeneous and included rats that did not show BBB dysfunction within the epileptogenic network ('healthy microvasculature') and rats who demonstrated diffused BBB dysfunction ('diffused microvascular pathology'), in both the 'epileptogenic' and the 'limiting' brain networks (Fig. 2C and D). Including both networks in the model resulted in sensitivity of 76.9% (10 of 13 epileptic rats were correctly classified) and specificity of 66.7% (three of nine non-epileptic rats were falsely classified) with AUC = 0.92 ($P < 0.0001$) in ROC analysis (Fig. 2E). Because one animal presented only one seizure, we further challenged our findings by repeating the analysis after reclassifying the animals into 'epileptic' and 'non-epileptic' to include this rat as 'epileptic'. Under these settings, early BBB damage in the piriform cortex was found again as a predictor for epilepsy ($\hat{\beta} = 1.676$). This model had sensitivity of 92.86% (13 of 14 epileptic rats were correctly classified) and specificity of 62.5% (three of eight non-epileptic rats were falsely classified) with AUC = 0.833 ($P = 0.004$) in ROC analysis.

To confirm the biopathological relevance of the proposed biomarker, histological analysis was carried in brains removed after MRI from naïve ($n = 4$) and at Day 2 following status epilepticus ($n = 4$, Fig. 3A). The piriform network showed a significant cellular loss in Cresyl violet staining (Fig. 3B), leakage of the serum proteins albumin and IgG, reactive astrocytes (using GFAP) and microglia (IBA-1) (Fig. 3C). Taken together, these findings confirm BBB dysfunction and associated neuroinflammation within the same brain regions identified in the MRI.

Isoflurane anaesthesia or losartan prevent microvasculopathy and epilepsy

To test the capacity of magnetic resonance-based identification of vascular pathology to not only diagnose the epileptogenic network and predict epilepsy, but also to follow-up response to treatment, we quantified magnetic resonance changes in animals treated with either isoflurane anaesthesia, a known suppressor of epileptiform activity (Prasad *et al.*, 2014; Tasker and Vitali, 2014) that was recently shown to prevent epileptogenesis in both the paraoxon and kainic models of epileptogenesis (Bar-Klein *et al.*, 2016), or losartan, an FDA-approved anti-hypertensive drug was shown to effectively prevent epileptogenesis induced by BBB dysfunction (Bar-Klein *et al.*, 2014*a*).

Anaesthetized animals ($n = 8$) underwent repetitive, 1 h sessions of deep anaesthesia (isoflurane, 1–2%), at 1, 6, 12 and 24 h following status epilepticus. Losartan was injected once every 24 h for the first 3 days (intraperitoneal, 60 mg/kg) and then added to the drinking water to complete 3 weeks of treatment (2 g/l). Video-ECoG monitoring was performed (Weeks 5–7 post status epilepticus, $n = 12$) to assess treatment outcome. Image analysis in both treatment groups, anaesthesia or losartan, did not reveal significant changes in signal in any brain region across time points (Fig. 4A). When compared to untreated animals, anaesthetized rats showed a significant reduction in T_2-weighted abnormal signals in the amygdala, corpus callosum, neocortex, pallidum, piriform network, septum and striatum at Day 2 ($P < 0.05$). Normalization of the T_2-weighted signals was also observed at 1 week (piriform network, septum, and striatum) and 1 month (amygdala, piriform network and striatum) after exposure ($P < 0.05$,

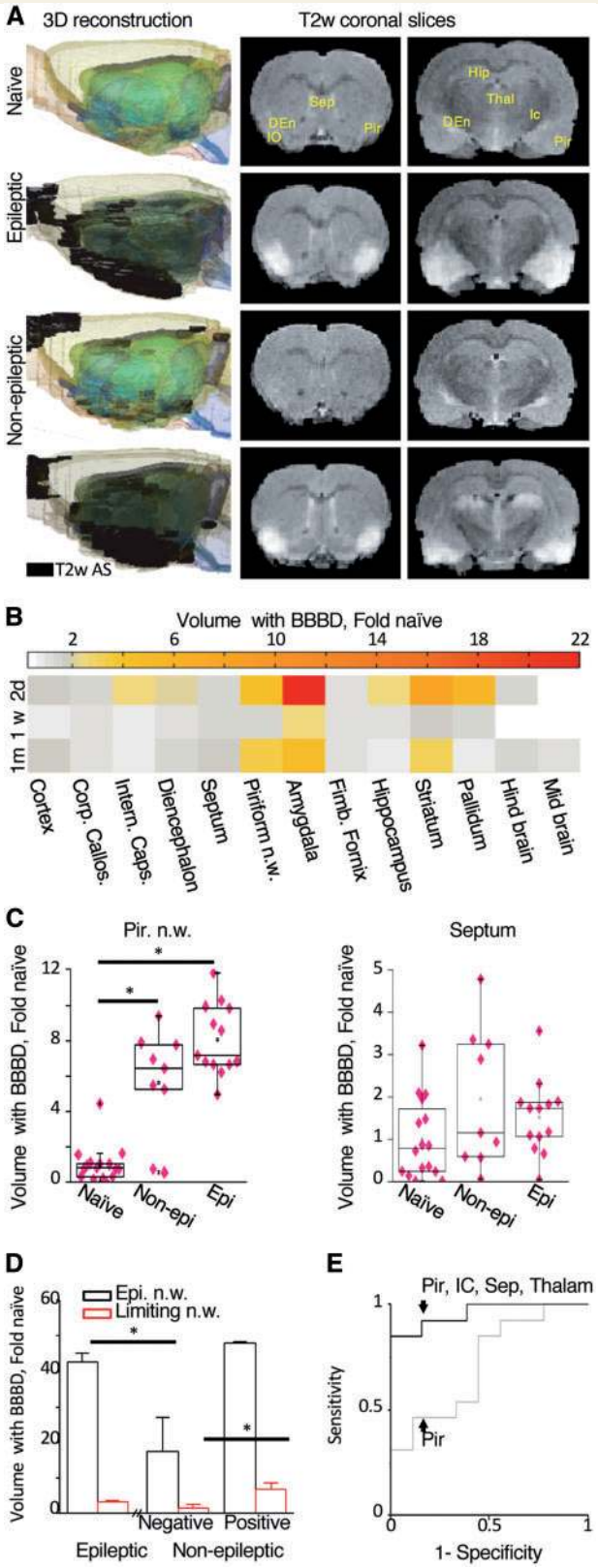

Figure 2 Imaging vascular integrity as a biomarker for epileptogenesis. (**A**) T_2-weighted scan-based 3D reconstructions (*left*) and coronal slices (*right*) of a control naïve, and three additional rats 2 days following status epilepticus, including a rat that later presented with seizures (epileptic) and two with no seizures (non-epileptic). Detected T_2-weighted abnormal signal (coloured in black in 3D images) is clearly observed in the epileptic rat. Status epilepticus-exposed non-epileptic rats were either 'negative' (i.e. did not show a significant signal change) or showed diffuse, severe damage (see text for details). (**B**) Fold change in T_2-weighted abnormal signal (compared to naïve controls) per region and

(continued)

Table 2). Losartan-treated rats similarly showed normalization of the signal at Day 2 in amygdala, corpus callosum, internal capsule, neocortex, midbrain, pallidum, piriform network and striatum ($P < 0.05$) and at 1 month in the amygdala, midbrain and piriform network ($P < 0.05$, Table 2). Importantly, while both treatments resulted in normalization of BBB integrity in the epileptogenic network (Fig. 4B), ECoG monitoring confirmed the magnetic resonance prediction with a reduction in the percentage of epileptic animals from 59.1% (13 of 22 non-anaesthetized rats) to 16.7% (2 of 12) in isoflurane-treated and 5.56% (1 of 18) in losartan-treated rats ($P = 0.02$ and $P < 0.0001$, respectively, Fisher's exact test, Fig. 4C).

Albumin-binding tracer shows increased magnetic resonance sensitivity to blood–brain barrier pathology

While T_1-weighted contrast enhancement is considered the most common approach for the detection of BBB dysfunction in clinical studies (Chassidim *et al.*, 2015), we found T_2-weighted signal changes more sensitive. As the choice of contrast agent may have a significant effect on the capacity to detect BBB damage, due to the nature of permeability changes (Kang *et al.*, 2013) and contrast agent pharmacokinetics, we also tested gadofosveset trisodium ($n = 6$), a clinically approved gadolinium-based albumin binding contrast agent that has a longer half-life in serum (Phinikaridou *et al.*, 2012). In non-exposed naïve rats with intact BBB, no difference between the two contrast agents was found in the extent of abnormal enhancement. However, after status epilepticus (1 h and 2 days) significantly higher percentages of voxels with abnormal enhancement were detected when the albumin-binding agent gadofosveset trisodium was used, compared to gadoteric acid ($P = 0.041$, $P = 0.023$, Mann-Whitney test, respectively, Fig. 5).

Discussion

A critical need in biomarker research is the development of animal models that, similar to the clinical condition, will show delayed complications (e.g. epilepsy) to a variable extent despite a similar insult, such that the sensitivity and specificity of the biomarker could be measured. We established a status epilepticus rat model for epileptogenesis using paraoxon, a commonly used organophosphate pesticide and an inhibitor of brain acetylcholinesterase. Paraoxon, likely due to massive increases in brain acetylcholine levels, triggers prolonged status epilepticus (Cehovic *et al.*, 1972; Marrs, 1993), which can be significantly shortened using the long-acting GABAergic agonist, midazolam. Using this treatment protocol epileptogeneiss is suppressed and delayed recurrent spontaneous seizures are recorded in <60% of the rats.

We evaluated microvasculopathy and damaged BBB by measuring the percentage of voxels in each of the 13 selected brain regions (comprising over 90% of brain volume) with a pathological T_2-weighted signal (for vasogenic oedema) (Gerriets *et al.*, 2004), T_1-weighted contrast enhancement (leakage of contrast agent through the dysfunctional BBB) (Chassidim *et al.*, 2013, 2015; Weissberg *et al.*, 2014) and diffusion weighted signal (for oedema) (Tomkins *et al.*, 2007; Chassidim *et al.*, 2013, 2015; Weissberg *et al.*, 2014). We found abnormal T_1-weighted contrast enhancement and T_2-weighted signals in suspected epileptogenic brain regions already 2 days after status epilepticus, throughout the epileptogenic period and after the establishment of epilepsy. Using a logistic regression model we identified an 'epileptogenic network', composed of the piriform network (including the olfactory bulbs, piriform cortex, dorsal endopiriform nucleus and inferior olive), which best predicts epilepsy. These results are consistent with previous studies showing that the same brain regions display the most robust inflammatory response in PET after pilocarpine-induced status epilepticus (Maeda *et al.*, 2003; Dedeurwaerdere *et al.*, 2012) and BBB breakdown after status epilepticus induced by kainic acid (van Vliet *et al.*, 2014, 2016*a*, *b*). The piriform cortex has a low threshold for seizures and seems to commence seizures in different models of epilepsy (Vismer *et al.*, 2015), possibly due to its tight connectivity with other epileptogenic brain regions, including the amygdala, hippocampus, entorhinal and perirhinal cortices (Löscher and Ebert, 1996). Exposure of the piriform cortex to a low dose of the GABA antagonist bicuculline results in bilateral clonic seizures (Piredda and Gale, 1985), and injection of gamma-vinyl GABA focally into the piriform cortex prevents seizures induced by systemic bicuculine (Piredda *et al.*, 1987). Interestingly, in a model of febrile status epilepticus in rat pups, T_2 relaxation time in the amygdala was reported to be reduced (Choy *et al.*, 2014), which may suggest different epileptogenic mechanisms in different developmental stages.

Figure 2 Continued

time in epileptic animals ($n = 13$). Note that regions showing increased signal at 1 month are already highlighted at Day 2 after status epilepticus. (**C**) Extent of BBB dysfunction (BBBD) in the piriform cortex and septum. Note the large variability within the exposed–non-epileptic (Non-epi) group. (**D**) The measured relative volume of brain regions with apparent BBB pathology in the epileptogenic and limiting networks in epileptic animals compared with non-epileptic non-responding (non-resp.) and responding (resp.) rats. (**E**) ROC analysis showing the specificity and sensitivity of the proposed biomarker using the piriform network only (grey line), and after adding the negative predicting value of the internal capsula, septum and thalamus (black line). DEn = dorsal endopiriform nucleus; Hip = hippocampus; IC = internal capsule; IO = inferior olive; n.w. = network; Pir = piriform cortex; Sep = septum; Thal = thalamus. *$P < 0.05$.

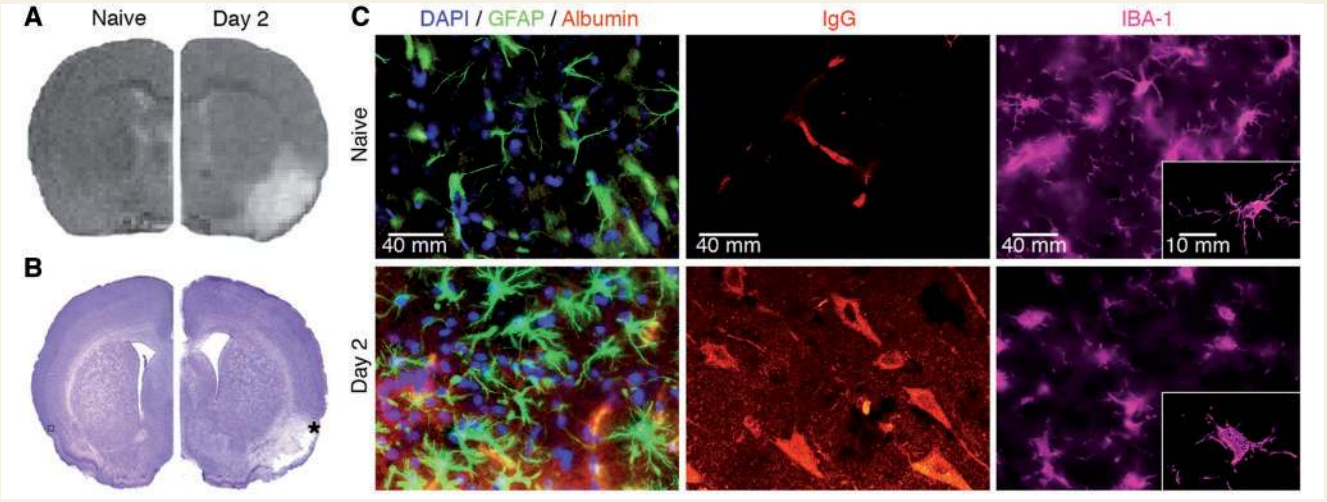

Figure 3 Magnetic resonance abnormal signal reflects neuronal damage, BBB dysfunction and brain immune response. (**A**) At Day 2 after status epilepticus, BBB lesion identified on T_2-weighted images reflects tissue damage observed with Cresyl violet staining (**B**). (**C**) Immunostaining within the peri-lesional piriform cortex (asterisk in **B**) against the astrocytic marker GFAP (green), serum albumin (red, *left*), IgG (red, *right*) DAPI (blue) and the microglial marker IBA-1 (magenta), showing extravasation of albumin and IgG with concomitant activation of astrocytes and microglia.

A striking unexpected observation was the identification of brain regions that, when affected, reduce the likelihood for the development of epilepsy after status epilepticus. Thus, status epilepticus-exposed non-epileptic animals could be stratified into 'negative' (rats that did not show microvasculopathy in the epileptogenic network) and 'positive' with diffuse magnetic resonance changes (microvasculopathy included the epileptogenic network, as well as the internal capsule, septum and thalamus). Whether the absence of seizures in this group is due to interrupted thalamocortical connectivity required for the spread of limbic seizures, as has been reported in temporal lobe epilepsy patients (He *et al.*, 2015), is yet unknown. This may be supported by a recent study demonstrating that rapamycin treatment results in reduced frequency of late seizures, while status epilepticus-induced damage and BBB pathology were aggravated (van Vliet *et al.*, 2016*a*,*b*). An alternative hypothesis is a true inhibition of the generation of seizures and/or generalization as reported (for example) for the substantia nigra pars reticularis in genetic absence epilepsy rats from Strasbourg (GAERS) (Akman *et al.*, 2015). Of interest is the involvement of the septal nuclei, with its reciprocal connections with olfactory and limbic structures, as well as the thalamus. Indeed, in brain slices from status epilepticus-induced epileptic rats septo-hippocampal cholinergic input to the entorhinal-hippocampal network has been shown to induce the generation of seizures (Zimmerman *et al.*, 2008).

The most common approach to directly measure leaky brain vessels is the use of T_1-weighted signal enhancement, following the injection of a gadolinium-based contrast agent. While in the present study T_2-weighted signal

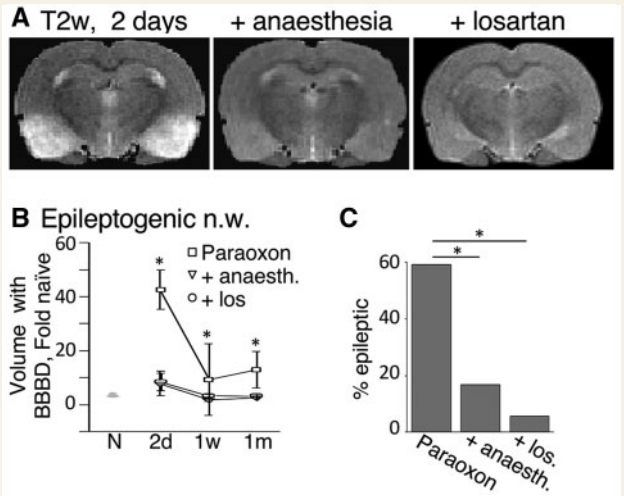

Figure 4 Repetitive anaesthesia and losartan treatment attenuates brain pathology in status epilepticus-exposed rats. (**A**) Representative T_2-weighted scans at Day 2 following insult from non-anaesthetized [(−) anes., *left*] from a rat that was provided with repetitive anaesthesia [(+) anaesthesia, *middle*] and from a rat treated with losartan [(+) losartan, *right*]. (**B**) Both repetitive anaesthesia and losartan treatment reduced significantly the volume of brain with apparent BBB dysfunction (BBBD) at Day 2, 1 week and 1 month ($P = 0.000$, $P = 0.007$, $P = 0.003$, and $P < 0.0001$, $P = 0.038$, $P = 0.001$, respectively, Mann-Whitney test) after status epilepticus. (**C**) Per cent epileptic animals in status epilepticus-exposed rats that were treated with paraoxon only compared to rats that were in addition exposed to repetitive anaesthesia (+ anesth.) or treated with losartan (+ los). Anaesthesia ($n = 12$) and losartan treatment ($n = 18$) showed a significant protective effect ($P = 0.02$, $P < 0.0001$, respectively, Fisher's exact test).

Table 2 Repetitive anaesthesia and losartan prevents brain abnormalities

Differences in brain magnetic resonance abnormal signals between treated and non-treated rats									
Brain region	**T_1-weighted contrast enhancement – anaesthesia**			**T_2-weighted abnormal signal – anaesthesia**			**T_2-weighted abnormal signal – losartan**		
	2 days	**1 week**	**1 month**	**2 days**	**1 week**	**1 month**	**2 days**	**1 week**	**1 month**
BBB dysfunction following status epilepticus									
Amygdala	ns	ns	ns	0.003	ns	0.008	0.008	ns	0.031
Corp. cal.	ns	ns	ns	0.005	ns	ns	0.023	ns	ns
Int. cap.	ns	ns	ns	ns	ns	ns	0.006	ns	ns
Midbrain	ns	ns	ns	ns	ns	ns	0.000	ns	0.031
Neocortex	ns	0.000	ns	0.005	ns	ns	0.013	ns	ns
Pallidum	ns	ns	ns	0.003	ns	ns	0.004	ns	ns
Piriform n.w.	ns	ns	0.032	0.011	0.013	0.000	0.023	ns	0.031
Septum	ns	ns	ns	ns	0.023	ns	ns	ns	ns
Striatum	ns	ns	0.032	0.000	0.013	0.002	0.000	ns	ns

A significance table showing statistically significant differences in magnetic resonance T_1-weighted contrast enhancement and T_2-weighted abnormal signals at Day 2 after status epilepticus between rats that were repetitively anaesthetised during the first 48 h after status epilepticus or provided with losartan treatment and rats that were anaesthetized for the first time at Day 2 (to perform magnetic resonance scans), by brain region (Mann-Whitney test with Benjamini-Hochberg false discovery rate correction). Brain regions with no significant differences in all time points were excluded from the table. Corp. cal. = corpus callosum; Int. cap. = internal capsule; Piriform n.w. = piriform network; ns = not significant (i.e. *P*-value > 0.05).

changes were found to better predict the development of epilepsy, T_1-weighted contrast enhancement abnormal signal was consistent with T_2-weighted changes and significantly higher within the epileptogenic network in treated rats (Fig. 2 and Table 1). We confirmed vascular pathology and leaky BBB using histopathological examination of Evans blue extravasation and positive immunostaining for serum albumin and IgG, and consistent with previous studies (Ding *et al.*, 2000; Ivens *et al.*, 2007; Tomkins *et al.*, 2007; Friedman *et al.*, 2009; Heinemann *et al.*, 2012), we show astroglial and microglia activation in regions with BBB dysfunction.

We next tested the potential of quantitative BBB imaging as a pharmacodynamics biomarker to follow-up treatment efficacy. Indeed, early treatment with either isoflurane anaesthesia or losartan prevented imaging changes within the 'epileptogenic network' and prevented epilepsy. Studying the mechanisms underlying the anti-epileptogenic effect of isoflurane anaesthesia is beyond the scope of the present study. The anti-epileptogenic effects of isoflurane have been recently shown in two independent models of epileptogenesis (Bar-Klein *et al.*, 2016) and are consistent with clinical data showing reduced mortality and morbidity in patients anaesthetized during pharmaco-resistant status epilepticus (Prasad *et al.*, 2014; Tasker and Vitali, 2014) and with the endothelial protecting and anti-inflammatory effect of isoflurane (Bakar *et al.*, 2012; Altay *et al.*, 2014; Bar-Klein *et al.*, 2016). Notably, high doses of isoflurane were previously shown to increase BBB permeability (Tétrault *et al.*, 2008), emphasizing the need for controlled, dose-response studies, but also a close, real-time monitoring of brain response to treatment.

Losartan has been recently shown to block epileptogenesis in animals following the induction of BBB breakdown or direct exposure of the neocortex to albumin (Bar-Klein *et al.*, 2014*a*). Interestingly, losartan was also shown to be anti-epileptogenic in the kainate model for epilepsy (Tchekalarova *et al.*, 2014). We now demonstrate the anti-epileptogenic effect of losartan in the status epilepticus model and suggest that early follow-up of microvascular pathology may predict such protective pharmacological effect.

Another question arising from our study pertains to the selection of imaging protocol and contrast agent for the identification of leakage through the compromised BBB. While abnormal T_2-weighted signal was found to better predict the development of epilepsy in our rat model, T_1-weighted contrast enhancement tests directly vessels' permeability and is thus expected to become a more specific biomarker for a compromised BBB as a specific pathobiological mechanism. The selection of contrast agent, route of administration, imaging protocol and magnetic strength will determine the extent of contrast accumulation and signal-to-noise ratio that allow the detection of abnormal signal. For example, it has been reported that a longitudinal (20 min) infusion of gadoteric acid overcomes the short serum half-life of the tracer and results in a significant increase in signals within brain areas with dysfunctional BBB (van Vliet *et al.*, 2014). We present an alternative approach by using gadofosveset trisodium, a gadolinium-based, FDA-approved tracer with a high affinity for serum albumin. To date there are no comparative human studies for the detection of the epileptogenic network using the two agents.

Finally, we propose a feasible contrast-enhanced modality to detect regions with BBB hyper-permeability in humans (Fig. 6). It is important to note that while quantitative monitoring of BBB pathology is not being routinely

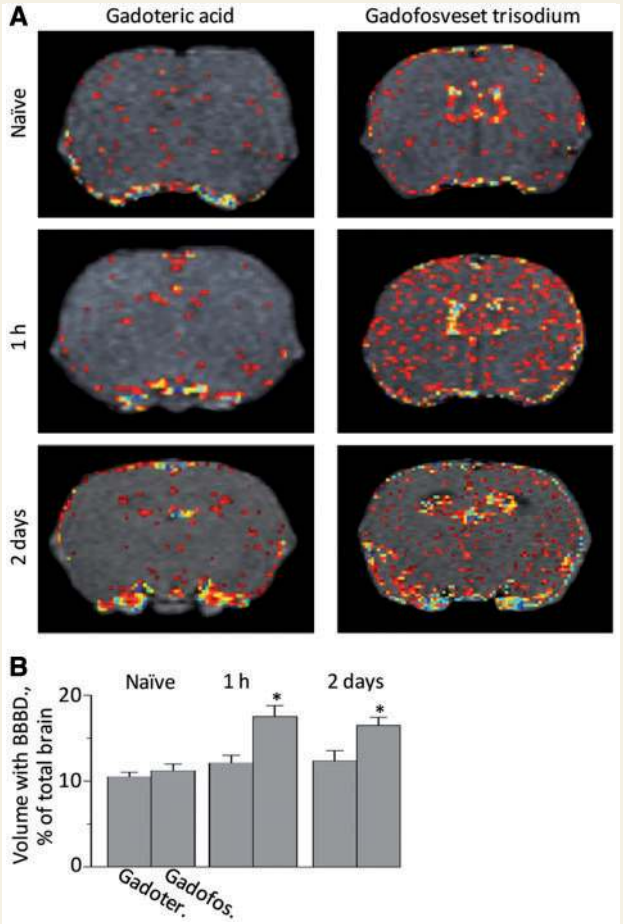

Figure 5 Albumin-binding tracer is more sensitive in detecting BBB dysfunction. (**A**) T_1-weighted images after injection of gadoteric acid (Gadoter) or the albumin binding tracer, gadofosveset trisodium (Gadofos), from naïve, 1 h and 2 days following status epilepticus. (**B**) Brain volume with abnormal enhancement showing higher detection of voxels with abnormal permeability when gadofosveset trisodium was injected compared to gadoteric acid at 1 h ($P = 0.041$, Mann Whitney test, $n = 6$ and 10, respectively) and 2 days ($P = 0.023$, Mann-Whitney test, $n = 8$ and 3, respectively), but not in naïve controls.

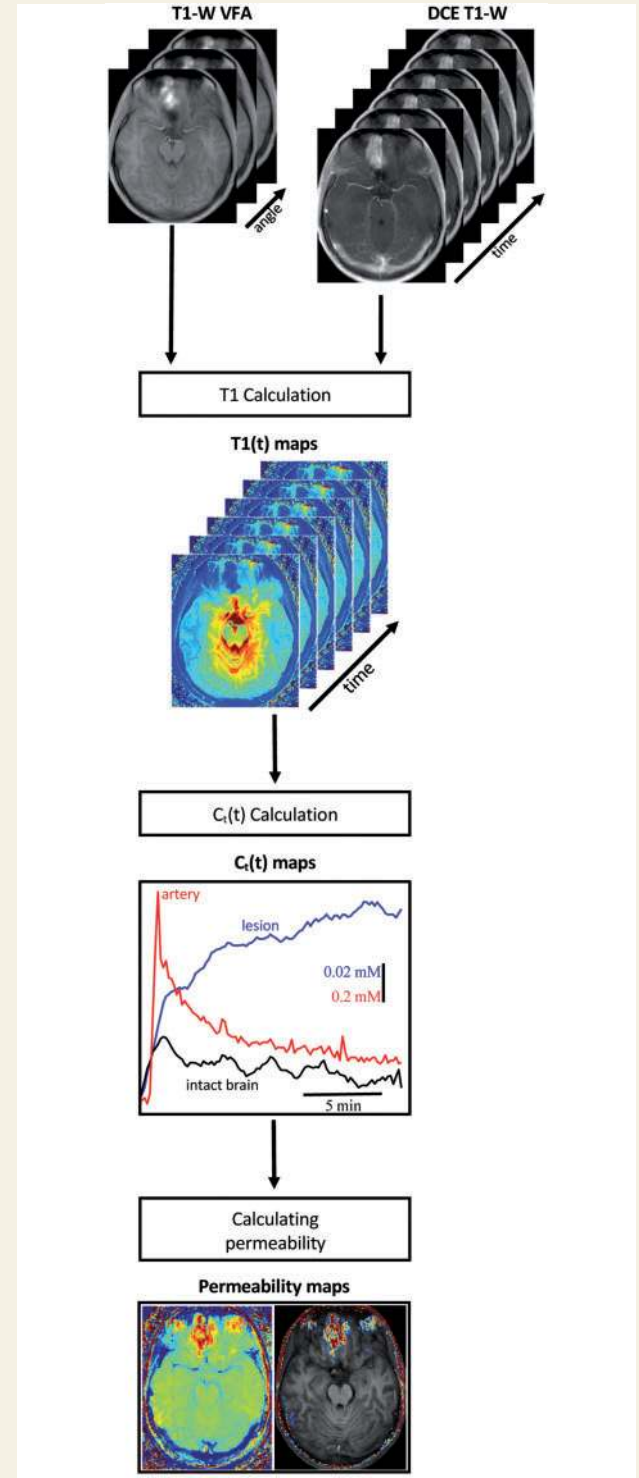

Figure 6 Imaging BBB dysfunction as a biomarker for epileptogenesis; outline for translation into the clinic. Two types of T_1-weighted sequences are used: (i) variable flip angle (VFA), used to generate preinjection T_1 maps; and (ii) dynamic contrast-enhanced (DCE) sequence, used to calculate T_1 map for each time point [$T1_{(t)}$]. Concentration curves [$C_{(t)}$] are generated and representative curves from artery (red), lesion (blue) and intact brain (black) are shown. BBB permeability map is calculated, and can be displayed on top of anatomical scan, using a population-based permeability threshold.

performed in the clinic, several groups have recently implemented contrast enhanced MRI to diagnose microvascular pathology in patients with mild traumatic brain injury (Weissberg *et al.*, 2014) and cognitive impairments of ageing (Zlokovic, 2008). Future studies are required to confirm the most sensitive, reliable and cost-effective protocol, and to test its value in predicting post-injury epilepsy in patients.

To conclude, we suggest quantitative MRI analysis of cerebrovascular dysfunction as a clinically applicable biomarker to diagnose the epileptogenic network. Large-scale studies are awaited to reveal the potential of BBB imaging as a diagnostic, prognostic and pharmacodynamic biomarker after brain injuries.

Funding

This study was supported by the European Union's Seventh Framework Program (FP7/2007–2013; grant agreement 602102, EPITARGET; A.F.), the NIH National Institute of Neurological Disorders and Stroke (RO1/NINDS NS066005, D.K., A.F.), the Israel Science Foundation (A.F.), the Medical Corps, Israeli Defense Forces, the CURE Epilepsy Foundation, the Nova Scotia Health Research Foundation and Canada Institute for Health Research (CIHR).

References

Abbott NJ, Rönnbäck L, Hansson E. Astrocyte-endothelial interactions at the blood-brain barrier. Nat Rev Neurosci 2006; 7: 41–53.

Akman O, Gulcebi MI, Carcak N, Ketenci Ozatman S, Eryigit T, Moshé SL, et al. The role of the substantia nigra pars reticulata in kindling resistance in rats with genetic absence epilepsy. Epilepsia 2015; 56: 1793–802.

Altay O, Suzuki H, Hasegawa Y, Ostrowski RP, Tang J, Zhang JH. Isoflurane on brain inflammation. Neurobiol Dis 2014; 62: 365–71.

Bakar AM, Park SW, Kim M, Lee HT. Isoflurane protects against human endothelial cell apoptosis by inducing sphingosine Kinase-1 via ERK MAPK. Int J Mol Sci 2012; 13: 977–93.

Bar-Klein G, Cacheaux LP, Kamintsky L, Prager O, Weissberg I, Schoknecht K, et al. Losartan prevents acquired epilepsy via TGF-β signaling suppression. Ann Neurol 2014a; 75: 864–75.

Bar-Klein G, Klee R, Brandt C, Brankstahl M, Tollner K, Dalipaj H, et al. Isoflurane prevents acquired epilepsy in two rat models of temporal lobe epilepsy. Ann Neurol 2016; 80: 896–908.

Bar-Klein G, Swissa E, Kamintsky L, Shekh-Ahmad T, Saar-Ashkenazy R, Hubary Y, et al. sec-Butyl-propylacetamide (SPD) and two of its stereoisomers rapidly terminate paraoxon-induced status epilepticus in rats. Epilepsia 2014b; 55: 1953–8.

Cacheaux LP, Ivens S, David Y, Lakhter AJ, Bar-Klein G, Shapira M, et al. Transcriptome profiling reveals TGF-beta signaling involvement in epileptogenesis. J Neurosci 2009; 29: 8927–35.

Campistol JM, Iñigo P, Jimenez W, Lario S, Clesca PH, Oppenheimer F, et al. Losartan decreases plasma levels of TGF-beta1 in transplant patients with chronic allograft nephropathy. Kindey Int 1999; 56: 714–19.

Cehovic G, Dettbarn W-D, Welscht F. Paraoxon: effects on rat brain cholinesterase and on growth hormone and prolactin of pituitary. Science 1972; 175: 1256–8.

Cendes F. Epilepsy in 2011: insights into epilepsy treatments and biomarkers. Nat Rev Neurol 2012; 8: 70–1.

Chassidim Y, Vazana U, Prager O, Veksler R, Bar-Klein G, Schoknecht K, et al. Analyzing the blood-brain barrier: the benefits of medical imaging in research and clinical practice. Semin Cell Dev Biol 2015; 38: 43–52.

Chassidim Y, Veksler R, Lublinsky S, Pell GS, Friedman A, Shelef I. Quantitative imaging assessment of blood-brain barrier permeability in humans. Fluids Barriers CNS 2013; 10: 9.

Choy M, Dube CM, Patterson K, Barnes SR, Maras P, Blood AB, et al. A novel, noninvasive, predictive epilepsy biomarker with clinical potential. J Neurosci 2014; 34: 8672–84.

David Y, Cacheaux LP, Ivens S, Lapilover E, Heinemann U, Kaufer D, et al. Astrocytic dysfunction in epileptogenesis: consequence of altered potassium and glutamate homeostasis?. J Neurosci 2009; 29: 10588–99.

Dedeurwaerdere S, Callaghan PD, Pham T, Rahardjo GL, Amhaoul H, Berghofer P, et al. PET imaging of brain inflammation during early epileptogenesis in a rat model of temporal lobe epilepsy. EJNMMI Res 2012; 2: 60.

Ding M, Haglid KG, Hamberger A. Quantitative immunochemistry on neuronal loss, reactive gliosis and BBB damage in cortex/striatum and hippocampus/amygdala after systemic kainic acid administration. Neurochem Int 2000; 36: 313–18.

Engel J, Pitkänen A, Loeb JA, Dudek FE, Bertram EH, Cole AJ, et al. Epilepsy biomarkers. Epilepsia 2013; 54 (Suppl 4): 61–9.

Friedman A, Bar-Klein G, Serlin Y, Parmet Y, Heinemann U, Kaufer D. Should losartan be administered following brain injury?. Expert Rev Neurother 2014; 14: 1365–75.

Friedman A, Kaufer D, Heinemann U. Blood-brain barrier breakdown-inducing astrocytic transformation: novel targets for the prevention of epilepsy. Epilepsy Res 2009; 85: 142–9.

Gerriets T, Stolz E, Walberer M, Müller C, Kluge A, Bachmann A, et al. Noninvasive quantification of brain edema and the space-occupying effect in rat stroke models using magnetic resonance imaging. Stroke 2004; 35: 566–71.

He X, Doucet GE, Sperling M, Sharan A, Tracy JI. Reduced thalamocortical functional connectivity in temporal lobe epilepsy. Epilepsia 2015; 56: 1571–9.

Heinemann U, Kaufer D, Friedman A. Blood-brain barrier dysfunction, TGFβ signaling, and astrocyte dysfunction in epilepsy. Glia 2012; 60: 1251–7.

Ivens S, Kaufer D, Flores LP, Bechmann I, Zumsteg D, Tomkins O, et al. TGF-beta receptor-mediated albumin uptake into astrocytes is involved in neocortical epileptogenesis. Brain 2007; 130: 535–47.

Kang EJ, Major S, Jorks D, Reiffurth C, Offenhauser N, Friedman A, et al. Blood-brain barrier opening to large molecules does not imply blood-brain barrier opening to small ions. Neurobiol Dis 2013; 52: 204–18.

Kenney K, Amyot F, Haber M, Pronger A, Bogoslovsky T, Moore C, et al. Cerebral vascular injury in traumatic brain injury. Exp Neurol 2016; 275 (Pt 3): 353–66.

Levy N, Milikovsky DZ, Baranauskas G, Vinogradov E, David Y, Ketzef M, et al. Differential TGF- signaling in glial subsets underlies il-6-mediated epileptogenesis in Mice. J Immunol 2015; 195: 1713–22.

Löscher W, Ebert U. The role of the piriform cortex in kindling. Prog Neurobiol 1996; 50: 427–81.

Maeda Y, Oguni H, Saitou Y, Mutoh A, Imai K, Osawa M, et al. Rasmussen syndrome: multifocal spread of inflammation suggested from MRI and PET findings. Epilepsia 2003; 44: 1118–21.

Marrs TC. Organophosphate poisoning. Pharmacol Ther 1993; 58: 51–66.

Oby E, Janigro D. The blood-brain barrier and epilepsy. Epilepsia 2006; 47: 1761–74.

Ongali B, Nicolakakis N, Tong X, Aboulkassim T, Papadopoulos P, Rosa-neto P, et al. Angiotensin II type 1 receptor blocker losartan prevents and rescues cerebrovascular, neuropathological and cognitive deficits in an Alzheimer's disease model. Neurobiol Dis 2014; 68: 126–36.

Phinikaridou A, Andia ME, Protti A, Indermuehle A, Shah A, Smith A, et al. Noninvasive magnetic resonance imaging evaluation of endothelial permeability in murine atherosclerosis using an albumin-binding contrast agent. Circulation 2012; 126: 707–19.

Piredda S, Gale K. A crucial epileptogenic site in the deep prepiriform cortex. Nature 1985; 317: 623–5.

Piredda S, Pavlick M, Gale K. Anticonvulsant effects of GABA elevation in the deep prepiriform cortex. Epilepsy Res 1987; 1: 102–6.

Pitkänen A, Löscher W, Vezzani A, Becker AJ, Simonato M, Lukasiuk K, et al. Advances in the development of biomarkers for epilepsy. Lancet Neurol 2016; 15: 843–56.

Prasad M, Krishnan PR, Sequeira R, Al-Roomi K. Anticonvulsant therapy for status epilepticus. Cochrane database Syst Rev 2014; 9: CD003723.

Racine RJ. Modification of seizure activity by electrical stimulation. II. Motor seizure. Electroencephalogr Clin Neurophysiol 1972; 32: 281–94.

Seiffert E, Dreier JP, Ivens S, Bechmann I, Tomkins O, Heinemann U, et al. Lasting blood-brain barrier disruption induces epileptic focus in the rat somatosensory cortex. J Neurosci 2004; 24: 7829–36.

Shrot S, Ramaty E, Biala Y, Bar-Klein G, Daninos M, Kamintsky L, et al. Prevention of organophosphate-induced chronic epilepsy by early benzodiazepine treatment. Toxicology 2014; 323: 19–25.

Tasker RC, Vitali SH. Continuous infusion, general anesthesia and other intensive care treatment for uncontrolled status epilepticus. Curr Opin Pediatr 2014; 26: 682–9.

Tchekalarova JD, Ivanova NM, Pechlivanova DM, Atanasova D, Lazarov N, Kortenska L, et al. Antiepileptogenic and neuroprotective effects of losartan in kainate model of temporal lobe epilepsy. Pharmacol Biochem Behav 2014; 127: 27–36.

Tétrault S, Chever O, Sik A, Amzica F. Opening of the blood-brain barrier during isoflurane anaesthesia. Eur J Neurosci 2008; 28: 1330–41.

Todorovic MS, Cowan ML, Balint CA, Sun C, Kapur J. Characterization of status epilepticus induced by two organophosphates in rats. Epilepsy Res 2012; 101: 268–76.

Tomkins O, Friedman O, Ivens S, Reiffurth C, Major S, Dreier JP, et al. Blood-brain barrier disruption results in delayed functional and structural alterations in the rat neocortex. Neurobiol Dis 2007; 25: 367–77.

Tomkins O, Shelef I, Kaizerman I, Eliushin A, Afawi Z, Misk A, et al. Blood-brain barrier disruption in post-traumatic epilepsy. J Neurol Neurosurg Psychiatry 2008; 79: 774–7.

Vismer MS, Forcelli PA, Skopin MD, Gale K, Koubeissi MZ. The piriform, perirhinal, and entorhinal cortex in seizure generation. Front Neural Circuits 2015; 9: 27.

van Vliet EA, da Costa Araújo S, Redeker S, van Schaik R, Aronica E, Gorter JA. Blood-brain barrier leakage may lead to progression of temporal lobe epilepsy. Brain 2007; 130: 521–34.

van Vliet EA, Otte WM, Gorter JA, Dijkhuizen RM, Wadman WJ. Longitudinal assessment of blood-brain barrier leakage during epileptogenesis in rats: a quantitative MRI study. Neurobiol Dis 2014; 63: 74–84.

van Vliet EA, Otte WM, Wadman WJ, Aronica E, Kooij G, de Vries HE, et al. Blood–brain barrier leakage after status epilepticus in rapamycin-treated rats I: magnetic resonance imaging. Epilepsia 2016a; 57: 59–69.

van Vliet EA, Otte WM, Wadman WJ, Aronica E, Kooij G, de Vries HE, et al. Blood–brain barrier leakage after status epilepticus in rapamycin-treated rats II: Potential mechanisms. Epilepsia 2016b; 57: 70–8.

Weissberg I, Veksler R, Kamintsky L, Saar-Ashkenazy R, Milikovsky DZ, Shelef I, et al. Imaging blood-brain barrier dysfunction in football players. JAMA Neurol 2014; 71: 1453–5.

Weissberg I, Wood L, Kamintsky L, Vazquez O, Milikovsky DZ, Alexander A, et al. Albumin induces excitatory synaptogenesis through astrocytic TGF-β/ALK5 signaling in a model of acquired epilepsy following blood–brain barrier dysfunction. Neurobiol Dis 2015; 78: 115–25.

Zimmerman G, Njunting M, Ivens S, Tolner E, Behrens CJ, Gross M, et al. Acetylcholine-induced seizure-like activity and modified cholinergic gene expression in chronically epileptic rats. Eur J Neurosci 2008; 27: 965–75.

Zlokovic BV. The blood-brain barrier in health and chronic neurodegenerative disorders. Neuron 2008; 57: 178–201.